A&A 520, A100 (2010)
DOI: 10.1051/0004-6361/200912996

Astronomy & Astrophysics

Acoustic waves in a stratified atmosphere

IV. Three-dimensional nonlinear hydrodynamics

W. Kalkofen[1,2], P. Rossi[3], G. Bodo[3], and S. Massaglia[4]

[1] Harvard-Smithsonian Center for Astrophysics, 60 Garden Street, Cambridge, MA 02138, USA
[2] Kiepenheuer-Institute for Solar Physics, Schöneckstr. 6, 79104 Freiburg, Germany
e-mail: wkalkofen@cfa.harvard.edu
[3] INAF Osservatorio Astronomico di Torino, Strada Osservatorio 20, 10025 Pino Torinese, Italy
e-mail: [rossi;bodo]@oato.inaf.it
[4] Università di Torino Dipartimento di Fisica Generale, via Pietro Giuria 1, 10125 Torino, Italy
e-mail: massaglia@ph.unito.it

Received 27 July 2009 / Accepted 8 March 2010

ABSTRACT

Context. The quiet solar chromosphere in the interior of supergranulation cells is believed to be heated by the dissipation of acoustic waves that originate with a typical period of 3 min in the photosphere.
Aims. We investigate how the horizontal expansion with height of acoustic waves traveling upward into an isothermal, gravitationally stratified atmosphere depends on the size of the source region.
Methods. We have solved the three-dimensional, nonlinear, time-dependent hydrodynamic equations for impulsively-generated, upward-propagating acoustic waves, assuming cylindrical symmetry.
Results. When the diameter of the source of acoustic waves is small, the pattern of the upward-propagating waves is that of a point source, for which the energy travels upward in a vertical cone, qualitatively matching the observed pattern of bright-point expansion with height. For the largest plausible size of a source region, i.e., with granular size of 1 Mm, wave propagation in the low chromosphere is approximately that of plane waves, but in the middle and upper chromosphere it is also that of a point source. The assumption of plane-wave propagation is not a good approximation in the solar chromosphere. The upward-directed energy flux is larger than that of the solar chromosphere, at least in the middle and upper chromosphere, and probably throughout.
Conclusions. Simulations of impulsively generated acoustic waves emitted from source regions with diameters that are small compared to the pressure scale height of the atmosphere qualitatively reproduce the upward expansion observed in chromospheric bright points. The emission features in the cores of the H and K lines are predicted to be blueshifted for a pulse and redshifted for the waves in its wake. The contribution of internal gravity waves to the upward energy flux is small and decreases with increasing size of the source region.

Key words. hydrodynamics – stars: late-type – waves – Sun: chromosphere

1. Introduction

Why is the solar chromosphere hotter than the photosphere? This question was first posed more than half a century ago (Biermann 1946; Schwarzschild 1948). While some progress has been made in answering the question, current research is still pursuing a complete explanation.

The chromosphere supports several wave types that may play a role in the dynamics and heating of the atmosphere. In the interior of supergranulation cells, where magnetic fields are weak, the possible types are acoustic waves and internal gravity waves. On the boundary of cells, where magnetic fields are strong and typically organized in magnetic flux tubes, they are longitudinal and transverse (kink) as well as torsional waves.

In the supergranulation cell interior, where the physics of the medium is the simplest, the magnetic field is weak and mainly horizontal (Lites et al. 2008). So it may be ignored in a discussion of chromospheric heating. Therefore, in the cell interior, acoustic waves and internal gravity waves are the only wave types that may be important. However, observations from space with the Transition Region And Coronal Explorer (Fossum & Carlsson 2005) and Hinode (Carlsson et al. 2007) have not found acoustic waves with sufficient energy flux to cover the observed radiation losses of the chromosphere. But internal gravity waves have been detected, possibly with sufficient energy flux to heat the internetwork chromosphere to the observed temperature (Straus et al. 2008).

It is not known, however, how these waves dissipate their energy. The heating of the solar chromosphere in the supergranulation cell interior is therefore an open problem. The dynamics, on the other hand, have been successfully simulated by Carlsson & Stein (1995, 1997) on the basis of acoustic waves with a one-dimensional radiation-hydrodynamic code where the driver at the lower boundary of the computational domain was the observed velocity field in a photospheric Fe I line (Lites et al. 1993). The simulations show conclusively that bright points are caused by acoustic shocks. But they also show two significant defects in the theoretical model: the simulated time-average

emission in the H_{2v} emission peak in the H line of Ca II fell short by a factor of 3 of the corresponding emission from the coolest of the empirical models of Fontenla et al. (1993), called FALA (cf. Carlsson & Stein 1995, Fig. 3), and, at the same time, the amplitude of the simulated temperature fluctuations exceeded the temperature difference between model FALA and the average model, FALC, by an order of magnitude – with a still greater difference in the corresponding H line intensities. Thus, the simulated time-average intensity of the Ca II emission from the middle chromosphere was much lower than observed, and the simulated maximal instantaneous intensity was much higher than observed.

Is it conceivable that a single explanation covers both the very low time-average emission and the very high instantaneous emission? The low time-average intensity in the theoretical model is consistent with the low flux of acoustic waves measured in space. But the high instantaneous intensity, as well as the large amplitude of its oscillations, requires a different explanation. The topology of wave propagation could, in principle, address both discrepant features of the simulations.

Our explanation of the large wave amplitude of the simulated chromospheric oscillations was in terms of the topology of wave propagation, where we assumed that the photospheric source region of the acoustic waves could be idealized as a point. The analytic solution of the hydrodynamic equations in three-dimensional (3D) space was for an isothermal, stratified atmosphere (Bodo et al. 2000) and for a perturbed atmosphere (Bodo et al. 2001). The solutions showed that the geometry of the space in which most of the wave energy propagated could be approximated by a cone, with its apex at the point source. The horizontal spreading of the wave front in upward propagation led to a more gradual growth of the wave amplitude than in one-dimensional (1D) propagation, with reduced dissipation at lower heights and more energy available for heating at greater heights (Kalkofen 2004). This would thus allow more acoustic energy to reach higher levels in the chromosphere and might explain the reduced emission in the h and k lines of Mg II that is found in the numerical solution of the 1D hydrodynamic equations for the chromospheres of late-type stars (Fawzy et al. 2002).

The aim of the present paper is to solve the 3D hydrodynamic equations numerically and to determine the geometry of the upward-propagating waves as a function of the size of the source region, varying it from the point source dealt with in our earlier, analytic, investigations, to the granular size that was investigated by Skartlien et al. (2000). In Sect. 2 we consider observational support for the proposition that the waves in the solar chromosphere behave like 3D waves emanating from a point source, in Sect. 3 we describe the numerical procedure, and in Sect. 4 we illustrate the numerical results for acoustic and internal gravity waves. In Sect. 5 we discuss the results in connection with the observed line shifts, and in Sect. 6 we draw conclusions.

2. Observations

The quiet, nonmagnetic solar chromosphere shows evidence of propagating acoustic waves in the form of spherical (3D) waves, both in the dynamics of 3 min oscillations and, less directly, in the heating. In the dynamics there are three indicators of 3D wave propagation: 1. the increase with height of individual regions oscillating with large amplitude at the acoustic cutoff period of 3 min; 2. the corresponding increase with height of the fractional area in the interior of supergranulation cells that oscillates with large amplitude; and 3. the relatively low shock strength compared to shocks of plane waves. In detail:

Table 1. Upward expansion of bright areas.

Height [Mm]	Diameter [Mm]	Reference
0	0.2	Sivaraman et al. (1990)
0.5	1	Foing & Bonnet (1984)
1	2	Cram & Damé (1983)
2	5	Carlsson et al. (1997)

1. In a typical supergranulation cell, which has a diameter of ca. 20 Mm, there are 10 to 20 bright features seen in the blue emission peaks in the cores of the H and K lines of Ca II, called H_{2v} and K_{2v} bright points, respectively (Brandt et al. 1992). Most of the H_{2v} bright points, which have a diameter of up to 2 Mm (Cram & Damé 1983) and are formed at a height of about 1 Mm in the chromosphere, are found above intergranular lanes in the photosphere (Sivaraman et al. 1990). The lanes have a width of 100 to 200 km. In the upper chromosphere, the oscillating regions have increased in size to 5 to 6 Mm (cf. Table 1). Although there are no simultaneous observations linking the oscillating regions in the middle layers of the chromosphere directly to those in the upper layers, the wave periods as well as the density of bright points observed or inferred in the two layers appear to be the same, which suggests that the oscillating regions refer to the same phenomenon (Kalkofen 2003). The height dependence of the diameter of bright points implies propagation channels in the shape of cones with an opening angle of about 90°.
2. In the middle layers of the chromosphere, at a height of 1 Mm, the filling factor of K_{2v} bright points is 5% to 10% of the area of the cell interior (von Uexküll & Kneer 1995); and in the upper layers, the fractional area of bright points, as observed in lines of neutral C, N, and O at a formation height of $z \approx 2$ Mm, has increased to 50% (Carlsson et al. 1997).
3. The observed temperature fluctuations at the acoustic cutoff period amount to only a few percent of the ambient temperature. For example, in the top layers of the chromosphere where the Lyman continuum is formed ($z \approx 2$ Mm), the temperature fluctuations are about 100 K (Wilhelm & Kalkofen 2003), and even the strongest K_{2v} bright points are observed to have shocks with peak brightness temperatures that are less than 30% above the ambient temperature (Liu 1974, Fig. 2). On the other hand, numerical simulations with plane acoustic waves by Carlsson & Stein (1995) show a temperature excursion at a height of 1.4 Mm from 3000 K to 16 000 K, and, at the top of the chromosphere, the temperature fluctuates maximally between 2000 K and 25 000 K (Carlsson & Stein 1994). Although their more recent calculations have a lower level of fluctuations because of a different boundary condition, the high simulated temperature excursions as compared to those observed highlight the effect of the assumed plane-wave propagation on shock strength. A plausible explanation of this difference between simulated and observed temperature variations is that the acoustic waves are not plane, but three-dimensional, and therefore spread the wave energy in the horizontal direction as they propagate in the vertical direction (Ulmschneider et al. 2005).

In chromospheric heating, the geometrical properties of the upward-propagating acoustic waves are not directly constrained by observations. Nevertheless, the relatively low level of temperature fluctuations implied by the fluctuations in the observed intensity of K_{2v} emission at random locations in the supergranulation cell interior (von Uexküll & Kneer 1995, Fig. 3) suggests 3D wave propagation and appears to exclude 1D wave propagation.

Thus, observations of phenomena in the nonmagnetic chromosphere that are associated with both the dynamics and the heating imply that the acoustic waves propagate upward as 3D waves, emanating from point-like sources in the photosphere. This 3D geometry of the dynamics of bright points is not surprising in view of the location of most wave sources in intergranular lanes. But for chromospheric heating, which we might imagine being caused by the emission of short-period acoustic waves by the Lighthill-Stein mechanism (Musielak et al. 1994), where the sources in the photosphere might then have granular size, i.e., with diameters of ∼1 Mm, this finding of 3D wave propagation is unexpected. But it might be consistent with the low value of the acoustic flux measured by Fossum & Carlsson (2005) and the very low value of the flux of high-frequency waves.

The wave generation discussed in previous work with plane waves indicated that impulsive excitation had the property of emitting a pulse that was followed by a wake at the acoustic cutoff period. The decay of the wave amplitude in the linear calculations resembled that of the solar phenomenon (Kalkofen et al. 1994; Sutmann & Ulmschneider 1995), but the nonlinear calculations showed decay that was faster than observed and, in addition, gave a very large wave amplitude for the first wave after the pulse, indicating again a problem with the plane-wave assumption or with the impulsive-excitation model.

An attempt to model nonplanar wave propagation was made by Skartlien et al. (2000) who assumed that the wave excitation was due to collapsing granules. Since the diameter of a granule, about 1 Mm, is comparable to the height at which the radiation in H_{2v} is formed, also 1 Mm, the departure from plane-wave propagation was minimal and essentially justified the plane-wave assumption. But, as explained above, solar observations suggest source regions with an area that is smaller than that of a granule by two orders of magnitude. We can therefore expect a calculation with a "point-like" source region to give the desired reduction in the wave amplitude as a function of height. At the same time, it should tell us whether impulsive wave excitation is a plausible mechanism.

3. The basic equations and numerical results

The hydrodynamic equations expressing the conservation of mass, momentum, and internal energy for a gravitationally stratified, isothermal atmosphere can be written as

$$\frac{\partial \rho}{\partial t} + \nabla \cdot (\rho \boldsymbol{v}) = 0$$

$$\rho \frac{\partial \boldsymbol{v}}{\partial t} + \rho(\boldsymbol{v} \cdot \nabla)\boldsymbol{v} = -\nabla p + \rho \boldsymbol{g} \qquad (1)$$

$$\frac{\mathrm{D}p}{\mathrm{D}t} - \gamma \frac{p}{\rho}\frac{\mathrm{D}\rho}{\mathrm{d}t} = (\gamma - 1)Q$$

where p, ρ, and $\boldsymbol{v}$ are, respectively, gas pressure, density, and velocity; $\boldsymbol{g} = \{0, 0, -g\}$ is the gravitational acceleration, and γ is the ratio of specific heats. The "artificial" heating-cooling term $Q \propto (T - T_0)^3$ is introduced to keep the background temperature constant (Kalkofen et al. 1994). We assume that the atmosphere is stratified in terms of plane layers, thus the equilibrium values of the unperturbed variables take the form:

$$p_0 = p_{00} \exp(-z/H),\ \rho_0 = \rho_{00} \exp(-z/H),\ v_0 = 0\,,\ \text{and}$$
$$T_0 = \text{const.},$$

where p_{00} and ρ_{00} are, respectively, the values of pressure and density at the reference height $z = 0$; $H = a^2/\gamma g$ is the pressure scale height, and $a = \sqrt{\gamma(p_0/\rho_0)}$ is the sound speed.

The numerical integration of the system (1) has been carried out using a PPM code (piecewise-parabolic-Method, Colella & Woodward 1984) in cylindrical coordinates, with the vertical axis ranging from –10 to 35 in units of the scale height and a uniform vertical grid of 2000 points (spacing of 2.25 km). The horizontal axis has a uniform grid from the central axis to a radial distance corresponding to 15 scale heights (spacing of 5 km), and then is stretched by a factor of 1.02 for consecutive grid points, up to a total width corresponding to 80 scale heights, for 500 grid points. We discuss the results between 0 and 20 scale heights in the vertical direction and 15 in the horizontal direction, although the actual calculation is spatially more extended to avoid reflection problems in the region of interest.

We consider a disturbance by a vertical velocity pulse of Gaussian shape with variable horizontal width, excited at the base of the atmosphere, in the form

$$v_z = \epsilon \exp\left(-\frac{(z - z_0)^2}{w_z^2} - \frac{r^2}{w_r^2}\right) \qquad (2)$$

where

$$w_z = 0.05H; \quad w_r = 0.05H,\ 0.5H,\ 5H.$$

The velocities v_z and ϵ are in units of the sound speed.

We consider three different values of w_r with the condition that the perturbation energy be the same, i.e.,

$$\epsilon\, w_r = \text{const.}$$

For 3D waves, the energy is partitioned between acoustic waves and internal gravity waves, whereas for 1D waves, which propagate only in the vertical direction, all energy goes into acoustic waves. In addition, for 3D waves, we have to consider the geometrical decrease of the wave amplitude as $\lesssim 1/r^2$, that dominates for $r \lesssim 2H$, and that this is important especially for the case $w_r = 0.05H$. Taking this into account, and the observational requirement of having strong shocks at $z = 15H$, we have chosen the constant to be equal to unity, which implies that $\epsilon = 20,\ 2,\ 0.2$, respectively, for the three cases considered.

3.1. Acoustic waves

Figure 1 shows the gray-scale spatial distribution of the thermal pressure, in units of the initial values, for the case $w_r = 0.05H$ and at the instant when the wave front has reached 15 scale heights. We see that the maximum value of the pressure is attained at the apex of the wave front, on the vertical axis, and that it declines off axis.

Figure 2 compares three waves in 3D having different radial extensions and amplitudes (but the same energy). The waves are excited by pulses and are seen at the time when the pulses have reached a height of 15 scale heights, which occurs at different times since the waves have different velocity amplitudes and therefore travel at different speeds. The first feature to note

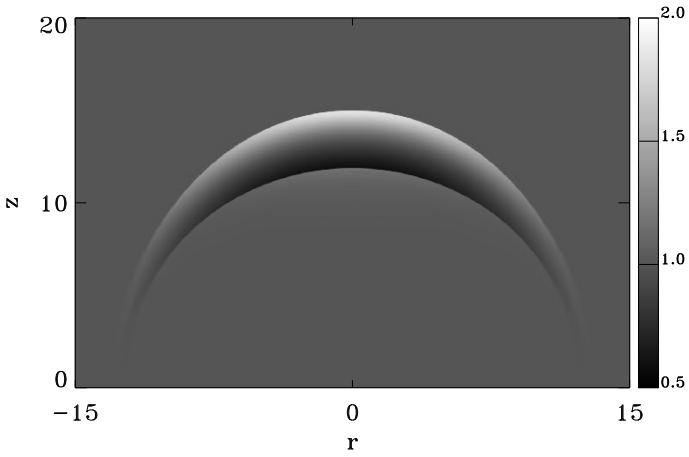

Fig. 1. Spatial distribution of the thermal pressure for $w_r = 0.05H$, in units of the values at $t = 0$, at the instant when the wave front has reached $15H$.

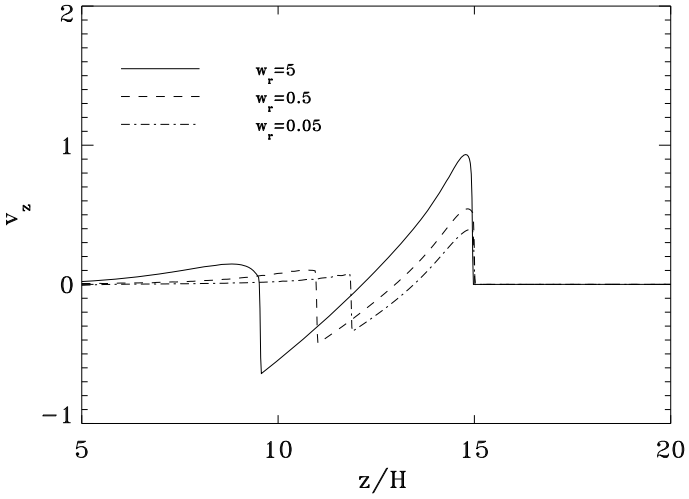

Fig. 2. Spatial behavior of the vertical velocity v_z versus height at the instant when the wave fronts have reached $15H$.

is that, going from extended to point source excitation, the wave shortens, i.e., the vertical distance between the pulse and the first maximum or minimum decreases. The separation between consecutive wave peaks in the $w_r = 5H$ case, which approaches the 1D limit, is nearly twice that of our most extreme 3D case, where $w_r = 0.05H$. This effect is related to the fact that in the former case, the first shock is stronger (at $z = 15$ H) and so the downflow is stronger and, as a consequence, the following shock stays far behind. Furthermore, looking at vertical velocity versus time at three different heights (Fig. 3), we see that at $z = 0$ the amplitude of the oscillation with $w_r = 0.05H$ is the highest but, with increasing height in the atmosphere, the wakes weaken. This effect comes from internal gravity waves (Bodo et al. 2000), which are not excited in 1D since they do not propagate in the vertical direction. At greater height ($z/H = 10$ and 15) the internal gravity waves disappear completely. The much more rapid decay with height and time of the wave from the "point-source" excitation, where $w_r = 0.05H$, is due to the more pronounced horizontal spreading in the vertical propagation of the wave.

The behavior of the wave velocity and amplitude may be easier to understand by looking, at given times, along the wavefront of the pulse to the radius where $P_{\rm wing}/P_{\rm apex} = 0.5$. One could compute a similar ratio at given heights but for different times (Bodo et al. 2001, Fig. 7). In Fig. 4, the thick solid line

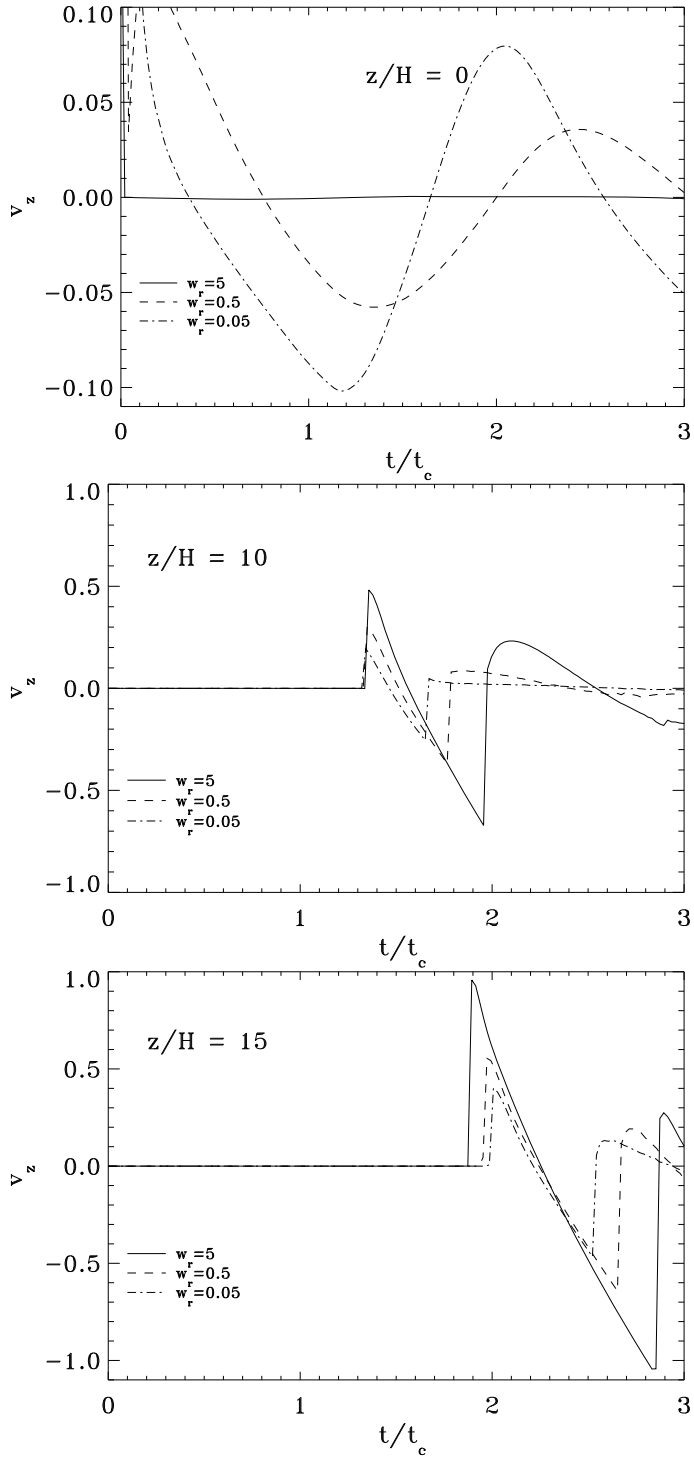

Fig. 3. Temporal behavior of the pulse amplitude v_z versus time relative to the acoustic cutoff period, t_c, along the z axis at different scale heights: $z/H = 0$ (*top panel*), $z/H = 10$ (*mid panel*) and $z/H = 15$ (*bottom panel*).

represents a propagation cone with an opening angle of 90°, i.e., the linear solution for a pulse perturbation emanating from a point source. The dot-dashed line is the horizontal size of a pulse with $w_r = 0.05H$. It shows the immediate flaring in 3D of the perturbation propagating up in the atmosphere, implying effectively a dilution of the energy from the beginning. Note that the feature visible within $2H$ for this case is not an artifact, but comes from the initial perturbation amplitude that is nonlinear and focuses the propagation cone before the conical

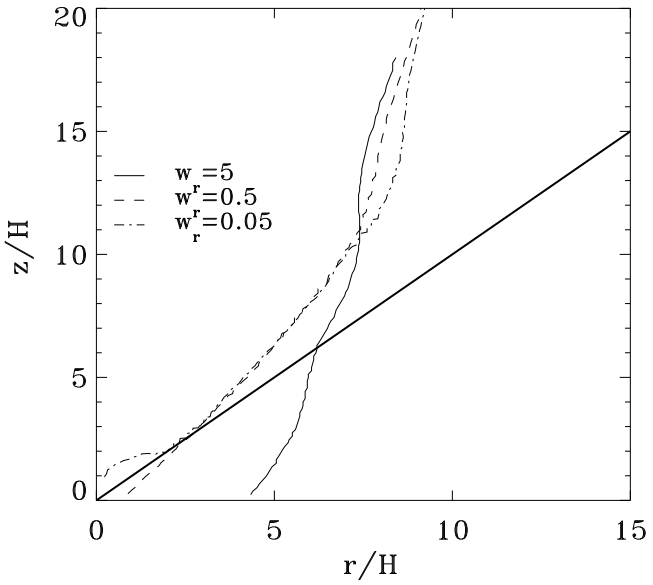

Fig. 4. Horizontal size of the perturbation for different w_r's. The size corresponds to $P_{\rm wing}/P_{\rm apex} = 0.5$. The plot should be read as r/H vs. z/H.

dilution of the wave can take place. Between 2 and 7 scale heights, the cases $w_r = 0.05H$ and $w_r = 0.5H$ (dashed line) maintain the same behavior, since their wave amplitudes are close in that height range. In contrast, in the case closest to the 1D case (solid, for $w_r = 5H$), the perturbation propagates essentially as a plane wave up to $5H$ but, when the shock-overtaking process becomes effective, starts to flare, however, never reaching the fully 3D transverse size. We can conclude that with the 3D approach the wake is strongly damped by the horizontal spreading of the wave energy. The impulsive excitation that seemed viable from 1D simulation is excluded by the 3D results since we no longer observe the wake. Our results give information on the wave propagation in an undisturbed medium: the extension of the perturbed region roughly follows a cone with a fixed opening angle. Starting from a perturbation with a horizontal size of more than $5H$ the 3D effects are negligible, at least up to the beginning of the shock-overtaking process, at which point the 3D case presents a flaring, with a consequent dilution, that does not occur in the 1D treatment.

3.2. Internal gravity waves

A point source perturbation impressed at the bottom of a stratified atmosphere gives rise to two kinds of waves: acoustic waves and internal gravity waves (Bray & Loughhead 1974). Following the linear analysis of Bodo et al. (2000), the two kinds of waves have the dispersion relations:

$$\omega_\pm^2 = \frac{1}{2}\left[(k^2+1) \pm \sqrt{(k^2+1)^2 - 16\frac{\gamma-1}{\gamma^2}k_x^2}\right]$$

where k_z, k_x are the wavenumbers in the vertical and horizontal directions, $k^2 = k_x^2 + k_z^2$, and the $\pm$ sign for the frequency ω refers to acoustic and gravity modes, respectively. Wavenumbers are in units of $1/2H$ and frequencies in units of the acoustic cutoff frequency $2\pi/P_{\rm ac}$, with $P_{\rm ac}$ the cutoff period. Bodo et al. (2000, Eq. (18)) have noted that the ratio of the internal energies of gravity to acoustic waves, in the linear limit, is zero for adiabatic perturbations and 1/3 for isothermal ones. Moreover, the energy flux of the two kinds of waves is proportional to their group velocities, whose vertical components are

$$(\boldsymbol{v}_{\rm g})_z = \frac{\partial\omega_\pm}{\partial k_z} = \frac{k_z}{2\omega_\pm}\left[1 \pm \frac{k^2+1}{\sqrt{(k^2+1)^2 - 16k_x^2(\gamma-1)/\gamma^2}}\right].$$

If one considers a propagation direction close to the vertical axis, one can compute the ratio of group velocities of gravity to acoustic modes. For example, setting $k_x = 0.1$ and $k_z = 1$, one derives a velocity ratio of about 5%. One can then conclude that the energy flux of gravity waves in the upward direction is small compared to the acoustic flux.

4. Discussion of the results

The aim of this paper is to study the topology of the wave propagation channel as a function of the size of the wave source. We chose three sizes, defined by the diameter of the source at the height at which the wave amplitude has dropped to half the peak value, i.e., the value on the symmetry axis: a "small" size of $d_1 = 10$ km at the height corresponding to unit optical depth in the continuum at 500 nm, $z = 0$; an "intermediate" size, of $d_2 = 100$ km at $z = 0$; and a "large" size, of $d_3 = 1$ Mm.

Interesting heights at which to determine the expansion of the propagation channel are the height corresponding to the base of the chromosphere, at $z = 0.5$ Mm, and the height of $z = 1$ Mm in the middle chromosphere, which is the approximate height of formation of the emission features of the blue peaks in the H and K lines of Ca II. We find that for the two smaller sizes, with $d = 10$ km and 100 km, the diameter of the propagation channel at $z = 0.5$ Mm has expanded by an order of magnitude, to 0.8 Mm; and for the largest source diameter, of 1 Mm, the channel has broadened by 20%, to 1.2 Mm. At the height of $z = 1.1$ Mm, all three channels have broadened to 1.5 Mm; and above 1.1 Mm, the three channels broaden together at a rate corresponding to that of a point source.

The width of the propagation channel is observationally defined not by the shape of the wave front at a given time, but by the passage of the wave through a given layer and, therefore, by optical depth, or height, in the atmosphere. Since we have shown in this paper that above $z = 1.1$ Mm the propagation channel resembles that of a point source, we can use the analytic results of Fig. 8 of Bodo et al. (2000) for a point source to estimate the increase in the diameter of a bright point and the corresponding reduction in the upward-directed wave flux. We find that, at a height of 1.5 Mm, the opening angle of the propagation cone for all three initial source diameters is about 130°, leading to the diameter of a bright point of 6 Mm at a height of 1.5 Mm in the upper chromosphere, with a corresponding reduction in the upward wave flux by a factor of 20 relative to the flux at 1 Mm height. It is interesting that the SUMER observations analyzed by Carlsson et al. (1997) show a bright point size in lines of neutral C, N, and O in the upper chromosphere of up to 8″, which agrees with the size we have estimated from our numerical solutions.

For a range of plausible sizes of bright points in the source layer, of 10 km to 100 km for a point source (Bodo et al. 2000), or for an extended, plane-wave source of 1 Mm (Skartlien et al. 2000), the solution in the middle to upper chromosphere resembles that of a point source, independent of the initial source size; and the substantial reduction in wave flux by the expansion of the propagation cone in large measure explains the large energy

flux in the 1D numerical solutions of Carlsson & Stein (1994, 1995) and others as compared to the energy flux in actual bright points.

A pulse launched in an undisturbed atmosphere travels upward, generating a strong downflow in its wake. Profiles of lines emitted by the pulse may exhibit a blueshift; the wave due to the wake will be strongly redshifted. However, in the solar chromosphere, the medium is not quiescent but in motion. A pulse could therefore show a redward or a blueward shift. But the wake should still result in a strong downflow. Profiles of lines emitted in the downflow will be strongly redshifted. We therefore expect that the most luminous bright points have the highest redshifts.

5. Conclusions

We have investigated the geometrical properties of acoustic-wave propagation in a stratified atmosphere with cylindrical symmetry and a constant scale height of 100 km. The waves were excited at the origin of the stationary medium by an energy pulse of constant value. The source region was described by a Gaussian shape with a diameter of $2w_r = 0.10$, 1.0, 10, measured in units of the scale height, and thus the diameter corresponded to 10 km, 100 km and 1000 km, respectively. These cases range from the width of intergranular lanes to the diameter of photospheric granules. The acoustic waves generated in the photosphere travel upward into the chromosphere in a propagation channel whose geometrical properties depend on the size of the source region, the initial wave amplitude, and the radiative losses due to the perturbation of the medium by the wave.

When the diameter of the source region is small compared to the thickness of the chromosphere and the initial wave amplitude is small compared to the sound speed, the waves travel in a cone whose opening angle is about 130° for a cone defined by a decrease of 50% of the pressure amplitude along the wave front. When the diameter of the source region is of granular size (1 Mm), wave propagation in the lower chromosphere resembles that of plane waves, with effects at the edge of the perturbed region playing a minor role, but in the middle and upper chromosphere, it resembles that of a point source. For the solar chromosphere, which has a thickness of 2 Mm, a wave with a value of the width parameter of $w_r = 5H$, corresponding to the diameter of a large granule with a diameter of about 1 Mm, would be well represented by a plane wave in the lower chromosphere, but with increasing corrections in upper layers. The observations discussed in this paper imply however that the acoustic waves responsible for bright points are best represented by waves emanating from small sources.

The generation of acoustic waves is accompanied by the emission of internal gravity waves (IGWs), whose contribution to the wave flux depends on the size of the source region. In a 1D medium, IGWs are entirely absent. Hence their contribution for a large source region with $2w_r = 1$ Mm is very small. For small source regions, idealized as point sources, the contribution to the energy budget of the solar atmosphere may be significant. However, their properties do not make it appear likely that they might be important for the wave flux in the middle and upper chromosphere. But the work of Straus et al. (2008) has shown that the energy flux in IGWs can dominate the one in acoustic waves and match the radiative losses in the lower chromosphere (up to ~600 km). Thus, while they might be important for heating the low chromosphere (where most of the energy is dissipated), their contribution to the dynamics and heating of the middle and upper chromosphere is likely to be small, and still needs to be investigated.

References

Biermann, L. 1946, Naturwissenschaften, 33, 118
Bodo, G., Kalkofen, W., Massaglia, S., & Rossi, P. 2000, A&A, 354, 296
Bodo, G., Kalkofen, W., Massaglia, S., & Rossi, P. 2001, A&A, 370, 1088
Brandt, P. N., Rutten, R. J., Shine, R. A., & Trujillo Bueno 1992, in Cambridge Workshop on Cool Stars, Stellar Systems and the Sun, ed. M. S. Giampapa, & J. A. Bookbinder (San Francisco: ASP), ASP Conf. Ser., 26 161
Bray, R. J., & Loughhead, R. E. 1974, The Solar Atmosphere (London: Chapman and Hall)
Carlsson, M., & Stein, R. F. 1994, in Proc. Mini-Workshop on Chromosph. Dynamics, ed. M. Carlsson (Oslo: Inst. Theor. Astroph.), 47
Carlsson, M., & Stein, R. F. 1995, ApJ, 440, L29
Carlsson, M., & Stein, R. F. 1997, ApJ, 481, 500
Carlsson, M., Judge, P. G., & Wilhelm, K. 1997, ApJ, 486, L63
Carlsson, M., Hansteen, V. H., de Pontieu, B., et al. 2007, PASJ, 59, 663
Colella, P., & Woodward, P. R. 1984, JCoPh, 54, 174
Cram, L., & Damé, L. 1983, ApJ, 272, 355
Fawzy, D., Ulmschneider, P., Stepien, K., Musielak, Z. S., & Rammacher, W. 2002, A&A, 386, 983
Fontenla, J. M., Avrett, E. H., & Loeser, R. 1993, ApJ, 406, 319
Foing, B., & Bonnet, R. M. 1984, ApJ, 279, 848
Fossum, A., & Carlsson, M. 2005, Nature, 435, 919
Kalkofen, W. 2003, Current Theor. Models and High-Res. Obs.: Preparing for ATST, ed. A. A. Pevtsov, & H. Uitenbroek, ASP Conf. Ser., 286, 443
Kalkofen, W. 2004, ed. A. K. Dupree, & A. O. Benz, IAU Symp., 219, 115
Kalkofen, W., Rossi, P., Bodo, G., & Massaglia, S. 1994, A&A, 284, 976
Lites, B. W., Rutten, R. J., & Kalkofen, W. 1993, ApJ, 414, 345
Lites, B. W., Kubo, M., Socas-Navarro, H., et al. 2008, 1237, ApJ, 672, 1237
Liu, S.-Y. 1974, ApJ, 189, 359
Musielak, Z. E., Rosner, R., Stein, R. F., & Ulmschneider, P. 1994, ApJ, 423, 474
Rammacher, W., & Ulmschneider, P. 1992, A&A, 253, 586
Schwarzschild, M. 1948, ApJ, 107, 1
Sivaraman, K. R., Bagare, S. P., & November, L. J. 1990, in Basic Plasma Processes on the Sun (Dordrecht: Kluwer), 102
Skartlien, R., Stein, R. F., & Nordlund, Å 2000, Apj, 541, 468
Straus, T., Fleck, B., Jefferies, S. M., et al. 2008, ApJ, 681, 125
Sutmann, G., & Ulmschneider, P. 1995, A&A, 294, 232
Ulmschneider, P., Rammacher, W., Musielak, Z. E., & Kalkofen, W. 2005, ApJ, 631, L115
von Uexküll, M., & Kneer, F. 1995, A&A, 294, 252
Wilhelm, K., & Kalkofen, W. 2003, 1137, A&A, 408, 1137